Overview of *Sloshel* project

L, Brosset[1], *Z, Mravak*[2], *M, Kaminski*[3], *S, Collins*[4], *T, Finnigan*[5]
[1]Liquid motion dept, Gaztransport & Technigaz, Saint-Rémy-lès-Chevreuse, France
[2]Marine Division, Bureau Veritas, Neuilly-sur-Seine, France
[3]Hydro Structural Services, MARIN, Wageningen, the Netherlands
[4] Shell International Trading and Shipping Company Limited, London, United Kingdom
[5] Chevron Energy Technology Co., San Ramon (CA), United States of America

ABSTRACT

This paper provides an overview of the Sloshel project, aspects of which are further described in other ISOPE 2009 papers (Kaminski, Bogaert, 2009; Malenica, Korobkin, Ten, Gazzola, Mravak, de Lauzon, Scolan, 2009; Maguire, Whitworth, Oguibe, Radosavljevic, Carden, 2009; Wang, Shin, 2009). The Sloshel project is a Joint Industry Project to collect data from full-scale sloshing experiments using unidirectional focused waves impacting on a fully instrumented LNG carrier NO96 membrane containment panel and a concrete block within a rigid vertical wall.

The paper sets out the relevance of the project within the overall methodology for the sloshing assessment of partially filled LNG tanks. It describes the experimental set-up, the parameters tested and numerical evaluation leading to new insights into the characteristics of LNG tank sloshing impacts and the influence of hydro-elasticity. The paper concludes with a summary of the numerical methods being developed and validated with this full-scale experimental data.

KEY WORDS: Sloshing, LNG, NO96, wave impact, gas pocket, Flip-Through, hydro-elasticity, Fluid-Structure Interaction, model tests, scaling laws, dimensionless numbers, numerical simulation, CFD

INTRODUCTION

Sloshing assessment of a membrane LNG carrier has traditionally been carried out using small-scale $(1:30 - 1:60)$ model tests, together with numerical simulations, and further supported by 40 years of operating experience. The global behavior of the liquid, which is ruled by Froude number, is the same at small scale and scale 1. This does not mean that the local behavior is also the same and that the impact pressures and durations obtained at small scale can simply be scaled by Froude/Euler scaling factors to full scale. Locally different phenomena, like the compressibility of the escaping or entrapped gas, are involved. These local phenomena may be ruled by other scaling laws than Froude and could be predominant.

Moreover, increasing demands for operational flexibility in LNG shipping and the development of an offshore LNG sector highlight the need for accurate prediction of sloshing effects in partially filled LNG tanks. This brings into question the accuracy of present experimental and numerical models for these conditions. To answer this question full-scale data are needed, with measurements of fluid dynamics as well as structural response.

Gaztransport & Technigaz, Bureau Veritas, MARIN and Shell initiated an ambitious Joint Industrial Project called *Sloshel*. The purpose was to design and perform tests in a large flume tank. These tests were designed to reproduce at full-scale the wave impact conditions that may occur in the tanks of LNG membrane carriers for low and partial fill conditions. Ecole Centrale Marseille, American Bureau of Shipping, Chevron, Lloyd's Register, Det Norske Veritas and Class NK joined the project at a later stage, thus building a very effective consortium that included the membrane designer, two major oil & gas companies, the five main class societies for LNG carriers, academia and a renowned marine research institute.

Unidirectional waves were generated by a wave-maker in a 240 m long open flume tank with a focusing process, so that they impact a 'rigid' wall on which a fully instrumented membrane NO96 containment system[1] had been mounted together with a rigid concrete block. A large database of measurements was gathered during 110 wave impacts.

At the same time theoretical and numerical developments were carried out in order to adapt the so-called generalized Wagner and Bagnold methods to simplified conditions idealizing typical impact patterns.

The project was designed to pursue the following objectives:

- Study the physics of wave impacts at full scale
- Study hydro-elasticity effects associated with the NO96 containment system
- Compare directly the structural response of the NO96 boxes to the loads
- Build a database for numerical validation
- Draw possible conclusions on the methodologies for sloshing assessment for both model tests and numerical simulations

TEST METHOD AND SET-UP

This section describes the Sloshel test method and setup. Kaminski and Bogaert (2009) give more details.

---

[1] GTT 'NO96' Membrane Tanks are prismatic in section and comprise a double barrier liquid-tight Invar membrane system, each barrier being supported on an insulation layer of plywood boxes filled with perlite. The plywood boxes are anchored to the ship's cargo hold through pre-tensioned couplers.

Test method

The Delta flume (NL), operated by Deltares was selected as the test facility. The open-air part of the flume is 5 m wide, 7 m deep and 240 m long. At one end of the flume there is a large piston of 800 kW power and 5 m stroke. A transverse vertical test wall, as shown in Figure 1, was placed at 143 m from the piston.

The process of generating a breaking wave by the wave focusing method, devised by Deltares, is illustrated in Figure 2. Using a second-order wave steering system, the piston generates successive waves of increasing lengths and heights. The wave train is generated in such a way that all waves add at one longitudinal position of the flume and produce a single, large breaking wave. The theoretical position where the waves meet is called the focal point. It is defined with reference to the front wall location.
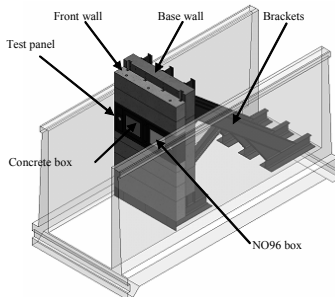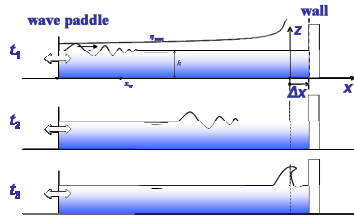

Fig. 1 - The test wall design   **Fig. 2** - Wave focusing process

Test Setup

The test wall is relatively stiff and rigid modular assembly consisting of a concrete front wall, a concrete base wall and three propped support steel beams (brackets). A steel test panel, able to accommodate two test pieces and associated instrumentation, was designed to be installed in the front wall at an adjustable height. As the test medium, water, has double the density of LNG, NO96 Standard *Reinforced* boxes (one primary and one secondary) were selected. These boxes and the instrumented solid concrete block were instrumented and sealed into the steel test panel. The front area of both tested structures was the same. Production-line Standard Reinforced NO96 boxes were obtained from a manufacturer in Spain. The consortium decided to test the NO96 boxes without their primary and secondary invar membranes. The boxes were not filled with the usual perlite granules. They were fixed to the test panel by use of four couplers in a similar way as on board LNG carriers. The complete wall has been designed in a massive way in order to separate its first modal frequencies from those of the NO96 boxes.

Instrumentation

Table 1 overviews the measured quantities and sensors. A state of the art, shock resistant, compact Data Acquisition System (DAS) for 300 channels with sampling rate of 50 kHz per channel was used. For determining the different types of impacts generated in the flume, MARIN developed an impact capturing matrix sensor (iCAM). The iCAM sensor consisted of a rectangular network (1.5 m x 3 m) of 640 single optical sensors able to distinguish air, aerated water and solid water. The iCAM sensor was placed on a longitudinal wall of the Delta flume just in front of the steel test panel.

The NO96 boxes were highly instrumented in order to measure both the hydrodynamic loads and the structural response. A lighter instrumentation was put on the concrete block for comparison and to check possible hydro-elasticity effects. The forces transmitted through both the NO96 boxes and the concrete block, were measured by means

of load cells located on the couplers and the force plate in between the tested structures and the steel test panel. Figure 3 shows a picture of the instrumented secondary NO96 box and a picture of the force plate.

Table 1.- Overview of instrumentation

Medium	Quantity	Sensor description
Water	Wave elevation	3 wave probes
		7 video cameras
	Wave velocity	5 video cameras (idem)
		iCAM (640 sensors)
	Impact type	
	Impact aeration	
NO96 box		
Interaction surface	Pressures	20 pressure gauges
	Velocities	20 accelerometers
Response	Strains	142 strain gauges
	Accelerations	24 accelerometers
Supporting structure	Forces	24 load cells
		4 couplers with load cells
	Accelerations	5 accelerometers
Concrete block		
Interaction surface	Pressures	10 pressure gauges
	Velocities	5 accelerometers
Supporting structure	Forces	24 load cells
		4 couplers with load cells
	Accelerations	5 accelerometers
Test panel		
	Pressures	2 pressure gauges
	Accelerations	3 accelerometers
Test wall		
Front wall	Pressures	11 pressure gauges
Base wall	Accelerations	8 accelerometers
Brackets	Forces	4 strain gauges

The whole chain of pressure measurement including pressure sensors and DAS was qualified in hydrodynamic conditions reflecting the highly dynamic nature of sloshing impacts.
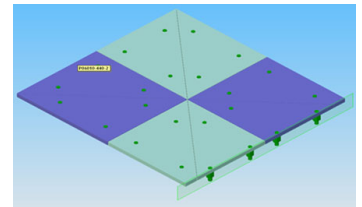

Fig. 3 -. Instrumented secondary NO96 box with its seven cells and force plate with load cells

TEST PROGRAM

A series of 110 full-scale tests were carried out. Different water depths ranging from 3.3 m to 4.25 m were used with two vertical locations of the panel (3.5 m and 4.5 m). For these different combinations, different shapes of breaking waves, associated with different focal point locations as shown in Figure 4, have been tested several times.
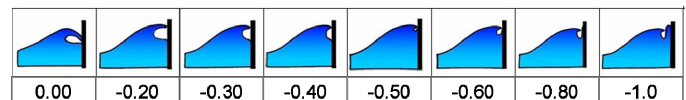

| 0.00 | -0.20 | -0.30 | -0.40 | -0.50 | -0.60 | -0.80 | -1.0 |

Fig. 4.- Shapes of breaking waves for different focal point locations

The simple classification using focal point location turned out not to be relevant. Wind was a partial cause of this, but the extreme sensitivity of certain types of impacts to the input conditions was the main reason. Nevertheless, the full-scale tests could be classified as shown in Table 2 based on the iCAM, video and pressure data.

Table 2. Overview of full scale tests

Impact type	Panel position	Water depth	Test numbers
Units-	m	m	-
Aerated Impact (AE)	3.5	3.50	4, 7, 10, 14, 18
	4.5	4.25	49, 61, 65
	4.5	4.00	86
Air Pocket Impact (AP)	3.5	3.50	2, 8, 15, 19, 20, 21, 22, 28, 29, 42, 43, 44, 45, 46, 47
	3.5	3.30	33, 36
	4.5	4.25	50, 58, 59, 60, 62, 63, 64
	4.5	4.00	66, 67, 68, 69, 70, 71, 72, 79, 80, 81, 89, 90, 91, 92, 93, 94, 95, 96, 98, 101, 102
Flip-Through Impact (FT)	3.5	3.50	1, 5, 11, 25, 26
	3.5	3.30	30, 31, 32, 34, 35, 37, 38, 39, 40, 41
	4.5	4.25	51, 52, 53, 54, 55, 56, 57
	4.5	4.00	73, 74, 75, 76, 77, 78, 82, 85, 88, 97, 99, 100, 103, 104, 107, 108, 109, 110
Slosh Impact (SL)	3.5	3.50	3, 6, 9, 12, 13, 16, 17, 23, 24, 27
	4.5	4.25	48
	4.5	4.00	83, 84, 87, 105, 106

These different types of impact are described in the next section. Figure 5 gives an example of a Sloshel impacting wave.
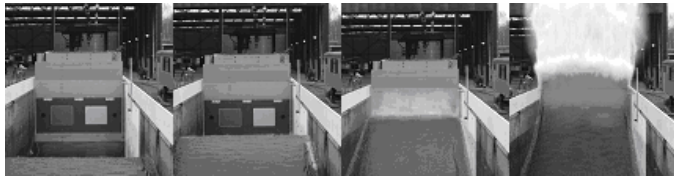

Fig. 5.- Example of a Sloshel full scale impacting wave

TEST RESULTS AND ANALYSIS

From the results of 110 wave impacts, a maximum pressure of 26 bars and a maximum force of 535 kN on the NO96 box were measured. The NO96 boxes were checked statically and dynamically after the tests and found to be intact and with the same properties.

The Sloshel database is very rich. A comprehensive analysis of the data is being carried out. This section describes only the first results and the preliminary analysis for both the loads and the structural response including hydro-elasticity.

The results presented refer to a restricted set of sensors: pressure sensors on the cover plate of the NO96 primary box and on the surface of the concrete block, accelerometers and strain gauges under the cover plate of the NO96 box just under the pressure transducers. These locations are numbered as shown in Figure 6.
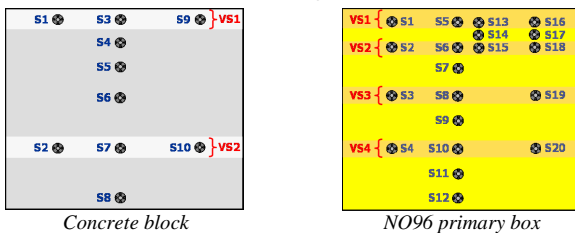

Concrete block	*NO96 primary box*

Fig. 6.- Sensor locations (pressure, accelerometers and strain gauges)

When describing pressures signals, reference is made to rise-time. This is defined as twice the duration between the half peak pressure and the peak pressure.

Main characteristics of the Sloshel waves

Four types of impacts have been defined according to their shape and loading characteristics (Kaminski and Bogaert, 2009).

Aerated impact (AE): the focal point is before the wall. The wave has already broken, entrapping an air pocket and generating many bubbles before hitting the wall. The maximum pressures are low, mitigated by the cushion of the air fraction. The compressibility of the air fraction makes the pressures oscillate but with different amplitudes for the different sensor locations. Such an impact is shown on Figure 7.
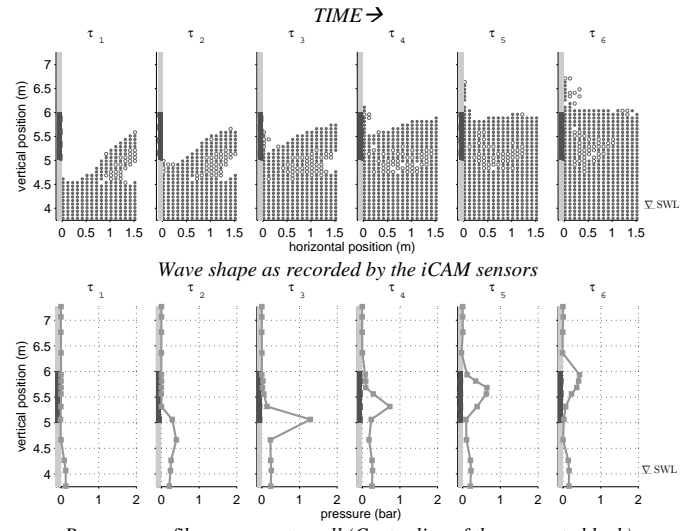

Wave shape as recorded by the iCAM sensors

Pressure profile on concrete wall (Center line of the concrete block)

Fig. 7.- Aerated impact (test 86).- Six instants, max pressure at τ_3, $\Delta\tau$=50 ms

Air Pocket impact (AP): focal point is closer to the wall. When approaching the wall the almost horizontal base of the wave runs up vertically along the wall, whereas the crest of the wave progresses horizontally. The speeds of the two phenomena are of the same order of magnitude. The wave is breaking onto the wall entrapping an air pocket in between its body and the wall. All sensors within the pocket observe the same oscillating pressure pulse. The period of the oscillations is related to the volume of gas entrapped. The pressures generated by the impact of the crest are higher and shorter than in the air pocket. The characteristic size of the air pocket is comparable to the size of the NO96 box (around 1 m). Such an impact is shown on Figure 8.
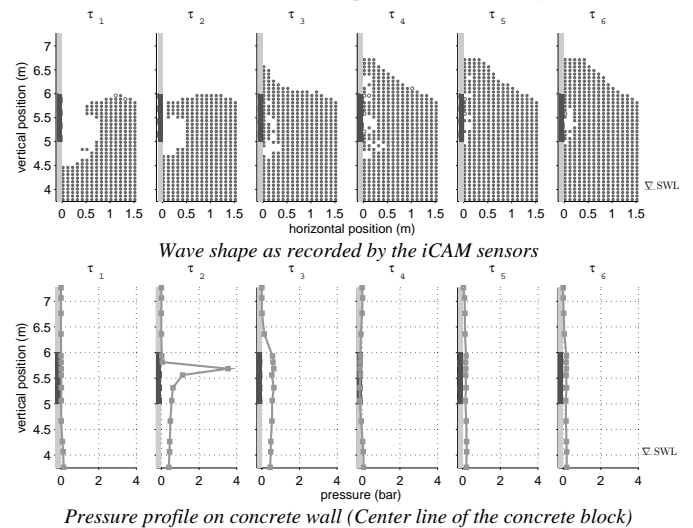

Wave shape as recorded by the iCAM sensors

Pressure profile on concrete wall (Center line of the concrete block)

Fig. 8. - Air pocket impact (test 79) - Six instants, max pres. at τ_2, $\Delta\tau$=50 ms

Flip-Through (FT): the focal point is a little behind the wall. This is a limiting case of the air-pocket impact for which the crest of the wave arrives late with regards to the run-up, so only a small air pocket may

be entrapped. A very intense vertical jet is expelled from the area when the pocket is collapsing. This type of impact leads to the highest pressures with the shortest rise-times. They are more localized with a characteristic size similar to the size of NO96 cells (around 10 cm, see Figure 3). Such an impact is presented on Figure 9.
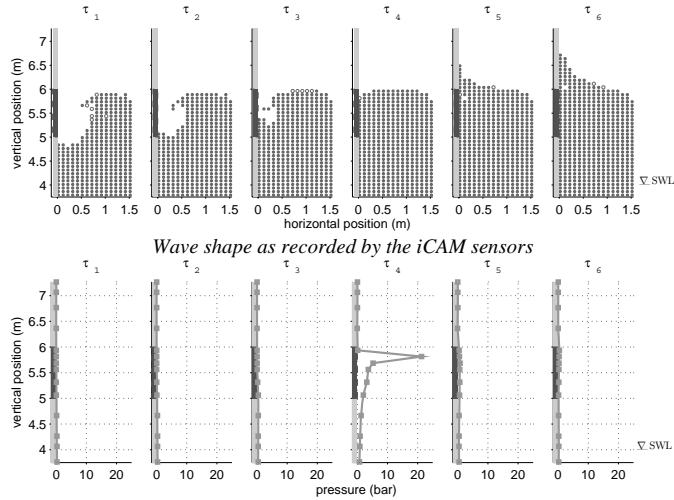

Wave shape as recorded by the iCAM sensors

Pressure profile on concrete wall (Center line of the concrete block)

Fig. 9. - Flip-Through (test 74) - Six instants, max pres. at τ_4, $\Delta\tau$=5 ms

Slosh impact (SL): when the focal point is even further downstream, the run-up is strong enough to prevent the wave breaking. The pressures are very low. Such an impact is shown on Figure 10.
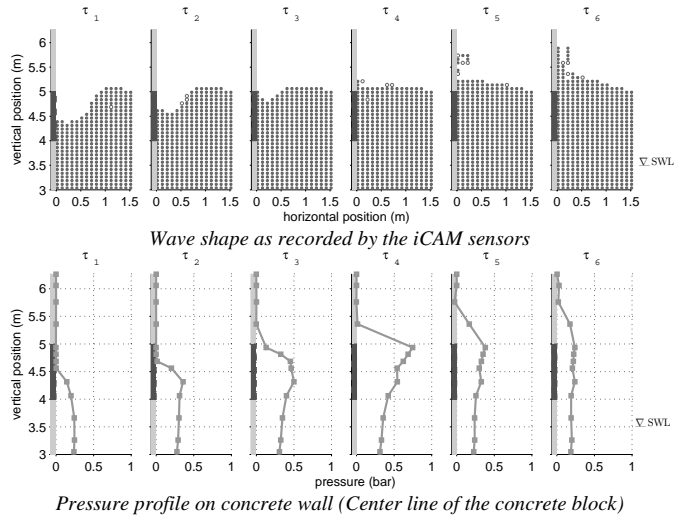

Wave shape as recorded by the iCAM sensors

Pressure profile on concrete wall (Center line of the concrete block)

Fig. 10 - Slosh impact (test 24) - Six instants, max pressure at τ_4, $\Delta\tau$=25 ms

The pressure pulses also have very different patterns in the time domain for the different impact types. Figure 11 shows examples of the pressure time series at the six sensor locations on the centre line of the concrete block (S3 to S8, Figure 6) for each impact type. It can be noted that the pressure gradient for the Flip-Through impact is more than 10 bar over the distance between two sensor locations (12.75 cm). The pressure pulse of the Air Pocket impact at S4 shows two superimposed different patterns: a sharp peak induced by the impact of the wave crest and a lower-frequency-content peak that is reproduced on all sensors, which is typical of the pressure within a compressed gas pocket. As expected, this peak presents some low frequency oscillations.

The characteristic size of the Flip-Through phenomenon is around 10 cm, which is very similar to the vertical size of a NO96 cell. This is

the same for the load induced by the wave crest of an air pocket impact when hitting the wall. So, the relevant loaded area to be considered for the structural response could be equal to the size of one cell.
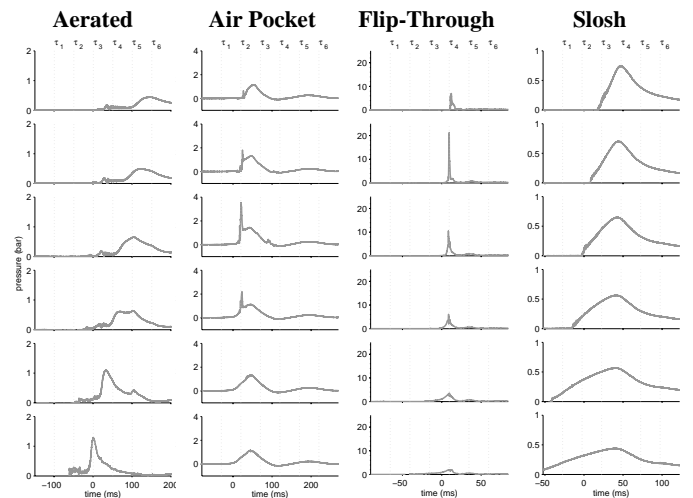

Fig. 11 - Pressure time series at six different heights on the centre line of the concrete block, for the different types of impacts

Therefore, for each Sloshel wave, the mean pressure on the six sets of sensors that are on the same horizontal lines for the NO96 box and for the concrete block (these sensors, shown on Figure 6 and named VS1 and VS2 on concrete block and VS1 to VS4 on NO96 box) has been calculated at each sampled time. Six new pressure signals have thus been obtained in this way for each Sloshel wave, as though six cell sensors had been used. These sensors are referred to later as Virtual Sensors (VS) and the pressures relating to VS are presented as $pressure^{VS}$, whereas the pressures relating to real sensors are presented as $pressure^S$.

There are too few impacts for each type to perform reliable statistics. So, Table 3 summarizes the main characteristics obtained by type of impact only for max value and mean of the max.

Table 3 - Main characteristics of the 110 Sloshel impacts on NO96 box

		AE	AP1 (1)	AP2 (2)	FT	SL
Pressure^S (bar)	Max	4.1	7.6	4.1	26	2.8
	Mean of max	2.6	3.2	2.1	8.0	1.3
Rise-time^S (ms)	Max*	1.0	0.1	12	0.24	14
	Mean of Max**	3.5	15	26	5.1	37
Pressure^{VS} (bar)	Max	2.7	4.3	4.1	14	2.5
	Mean of Max	1.7	2.3	2.0	5.4	1.2
Rise-time^{VS} (ms)	Max*	3.5	6	12	0.6	15
	Mean of Max**	7.5	21	25	6.8	30
Force (kN)	Max	65	343	-	534	195
	Mean	52	176	-	280	90

* For the rise-times, Max* denotes the rise time of the max pressure
** For the rise-times, Mean of the Max** denotes the mean rise-times of the max pressures for the different waves
(1) For AP1 (air pocket), the overall max values are shown in the table
(2) For AP2 (air pocket), max values within the air pocket are shown in the table

The comparison between the values obtained on the one hand at the sensor level (S) and on the other hand at the cell level (VS), gives an idea of the three-dimensional effects. Indeed, if the wave were ideally two-dimensional, these values would be the same. Column AP2, giving the results exclusively from sensors within air pockets, presents almost the same values for $pressure^S$ and $pressure^{VS}$, which shows a two-dimensional behaviour of the air pockets. The Flip-Through impact pressure pulses with the highest peak pressures on the smallest loaded areas have also the shortest rise-times.

How representative of Sloshing waves are the Sloshel waves?

Membrane LNG vessels have a tank height H ranging from 17 m to 29.2 m. The water depth studied during Sloshel project ranges from 3.3 m to 4.25 m. This corresponds to a range of filling ratios from 11.3%H to 25%H that includes those for which the highest pressures are recorded during sloshing model tests for conventional ship dimensions (around 20%H).

According to sloshing model tests, for these fill levels and when the significant sea wave height is large enough (larger than 1.5 m) to induce travelling waves within the tank, the wave system is always composed of transverse travelling waves, whatever the relative heading between the sea and the ship. Figure 12 shows such travelling waves recorded during sloshing model tests in GTT.
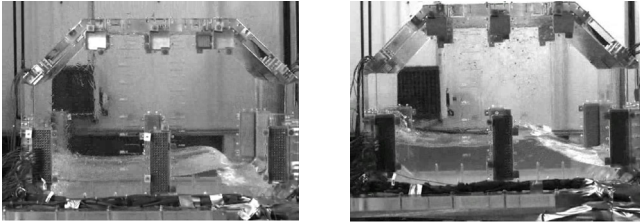
Fig. 12 - Typical travelling waves obtained during sloshing model tests at GTT for low or partial fill levels. Left: 15 %H, Right: 25 %H

The waves break more or less close to vertical walls. So, by tuning the focal point location of a breaking wave train in a flume tank, relevant impact situations can be studied.

Sloshing model tests for sloshing assessment are performed in 3D with irregular motions. So, capturing the patterns of the impacts by video leads to disappointing results. Figure 13 shows some impacts captured during 2D sloshing tests performed by GTT for R&D purpose.
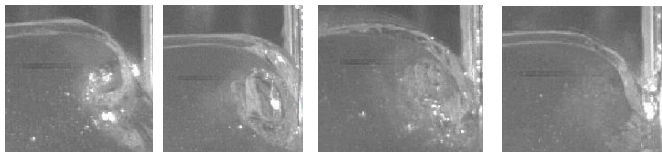

Fig. 13 - Sloshing Impacts during 2D sloshing model tests (GTT)

Aerated, Gas Pocket or Slosh kinds of impacts are clearly present during sloshing model tests. Aerated and Slosh are the types that do not require a precise focus with regard to the wall impacted. So they are the most frequent type. Flip-Through impacts, on the other hand, require precise focus and it is not clear how frequent they are during 3D model tests with irregular motions.

Differences between the Full-Scale Sloshel waves and the real sloshing waves within LNG tanks might exist, coming from the 2D simplification, the inertial accelerations of the ship or the gas condensation. Nevertheless, the Sloshel wave impacts are considered as particularly relevant for a better understanding of sloshing impacts.

Repeatability, sensitivity, variability

An important result of Sloshel project has been to better understand the high sensitivity of liquid impact loads to input conditions. Even though in an open-air flume, the wind had necessarily a bad influence, Figure 14 illustrates that the wave elevation repeated pretty well for the same signal of the piston. The curves correspond to the tests 73 to 77. They all have been classified as Flip-Through type and include the highest pressure recorded.

The largest absolute difference on the maximum amplitude is approximately 1 cm. This is a good performance recognising that the wave is 1.5 m height for a 4 m depth and has run 116.1 m from the paddle to that point. This performance characterizes the repeatability of

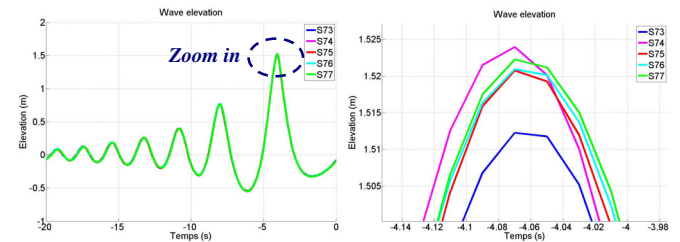the global flow, which is the input condition for the impacts.

Fig. 14 - (Left) Wave elevation at a wave gauge located at 26.9 m of the wall for 5 similar waves (tests 73 to 77). (Right) Zoom on the crest

Nevertheless, the parameters characterizing the impact loads and structural response show much worse repeatability. Figure 15 shows these discrepancies by scatter plots of different parameters measured on the NO96 box versus the focal point. The different types of impacts are represented by different symbols of different colours.

The high variability is not only observed for very local parameters such as the maximum pressures measured by the pressure transducers. Integrated values like max pressures on the cells or global force behind the NO96 box also show a high variability. Consequently the response of the structure also shows the same trend.
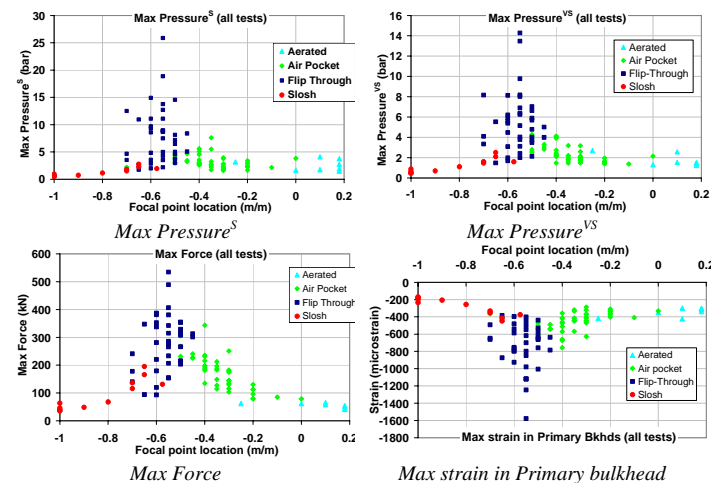

Max Pressure^S   *Max Pressure^{VS}*

Max Force   *Max strain in Primary bulkhead*

Fig. 15 - Scatter plots for different parameters of the NO96 box vs. focal point location.

The Flip-Through - the most localized type of impact - leads to the highest variability. This high variability of the local impact parameters for repetitive and simple global impact conditions explains the high variability obtained during 3-D sloshing model tests for more complex conditions. It is difficult to imagine how numerical simulations could be able, at short or medium term, to reproduce in detail the complex local phenomena involved during these sloshing impacts. A specific strategy needs to be defined to ensure relevant application of numerical simulations.

Structural response of the NO96 boxes

In this sub-section the dynamic response of the NO96 boxes is addressed directly by comparison between loads and strains. A potential amplification or filtering of the structural response, depending on the rise-time, with regards to the quasi-static behaviour is being tracked.

The NO96 Containment System has different Structural Limit States (SLS) that need to be checked during a sloshing assessment. Figure 16 (left) summarizes the three main SLS for NO96.
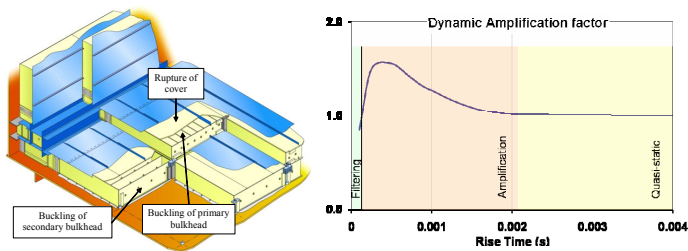
Fig. 16 - (Left) The three main Structural Limit States of NO96 (Right) Example of DAF curve vs. rise-time for a given size of the loaded area

These SLS have very different consequences when the load exceeds the limit. The slight damages that were observed in 2006 on board a NO96 ship and described by Yataghene & Gavory (2008) correspond to an excess of the cover plate bending limit when standard boxes with single 12 mm thick cover were used. The consequences of this failure mode, although annoying for the owner, will not lead to major damage. The risks related to a bulkhead rupture would be higher. Accordingly the designer keeps the SLS of the cover plate as a weak point. So, the results presented in this sub-section are focused on the cover plate SLS.

Several methodologies for sloshing assessment use Dynamic Amplification Factors (DAF) as a function of rise-time and size of loaded area, to account for the real dynamic behaviour of the insulation system. Figure 16 (right) presents such a DAF curve with regards to the rise-time for a given size of the loaded area. Regarding the bending of the double cover plate, the maximal DAF is obtained for a rise time between 0.25 ms and 0.75 ms corresponding to the maximum bending response of the cover-plate in between two bulkheads.

Considering all 20 sensor locations of the cover plate one by one, the scatter plots of maximum strains vs. maximum pressures have been plotted. The quasi-static behaviour of the cover plate appears clearly for low pressures and long rise times. A line can be plotted from these points for each sensor. One possibility is that points which are scattered from this line are affected by dynamic effects. Figure 17 (left) shows such scatter plot for sensor 6 (see Figure 6), which is located where the most violent impacts occurred. A few points, corresponding to high pressures and short rise-times are below the curve, but actually for other sensors the opposite is also true.

The maximum strain under the cover plate for a cell is not only influenced by local pressures but also by the mean pressure on the cell. Figure 17 (right) shows the same kind of scatter plot (Maximum strain vs. Maximum pressure) for the Virtual Sensor 2 that covers the cell including the Sensor 6 (see Figure 6).
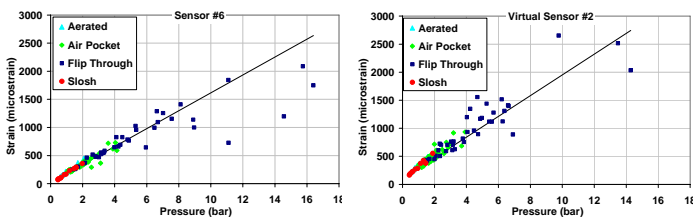

Fig. 17 - Scatter plot maximum strain vs. maximum pressure for Sensor 6 (left) and for Virtual Sensor 2 (right)

A linear behaviour for low pressures and long rise-times is still present but the behaviour for the high pressures looks significantly different than for the local sensor. Such a figure must be analysed carefully. Indeed the differences with regards to the straight line can be explained by other factors than a dynamic effect. The distribution of pressures on the cell at same mean pressure is of importance. Moreover dynamic effects can be induced not only by short rise-times, but also by pressure pulse travelling.

In summary, conclusions cannot be drawn on the relevance of DAF application from simple analysis. Systematic Finite Element Analysis is being done to derive reliable conclusions.

Hydro-elasticity

The Sloshel test panel has been designed especially to enable the comparison between the response of a solid concrete block (considered as rigid) and NO96 response in the same conditions. Unfortunately, phenomena inducing the highest pressures like the Flip-Through or the impact of the crest of a breaking wave are much localized and never develop in a perfect bi-dimensional way, which makes the comparison difficult. Indeed the spreading of the maximum pressures on a horizontal line of the wall, due to the sensitivity of such phenomena to input conditions, is more important that the amplitude of the effect (hydro-elasticity) that is intended to be detected.

Figure 18 illustrates this fact. It shows, on the left, pressure pulses for test 99 (Flip Through) recorded by sensors 2, 6, 18 on NO96 and sensor 4 on the concrete block, on the same horizontal line. It shows, on the right, pressure pulse for test 108 (FT) recorded by sensors 1, 5, 16 on NO96 and sensor 3 on concrete, on the same level.
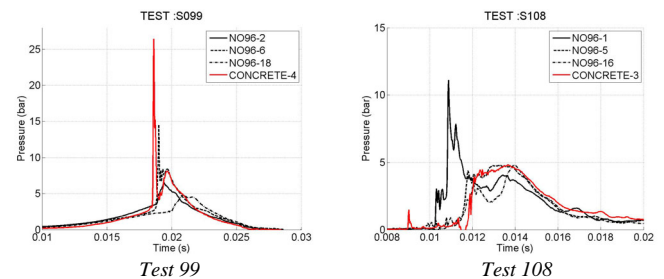
Test 99 | *Test 108*
NO96 S2, S6, S18 –Concrete block S4 | NO96 S1, S5, S16 – Concrete block S3

Fig. 18 – 3D effects – Pressures on sensors at same horizontal line

It is especially clear for test 108 that difference between red and black curves is not due to hydro-elasticity but to local different conditions. Thus, only a statistical comparison between results on NO96 box and concrete block might be relevant for detection of possible hydro-elasticity effect.

There is not the same number of pressure sensors on the NO96 box (20) and the Concrete block (10). This could bias statistical results if comparisons were made on all sensors. So, Figure 19 shows now the Joint Probability Density Functions (max pressures/rise-times) on Concrete block and NO96 box for all tests but for only the ten sensors at similar locations (see Figure 6).
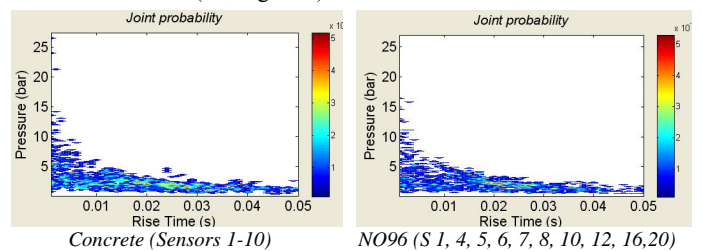

Concrete (Sensors 1-10) | *NO96 (S 1, 4, 5, 6, 7, 8, 10, 12, 16,20)*

Fig. 19 - Joint Probability Density Functions (max pressure – rise-time) for all tests on concrete block (left) and NO96 box (right)

There is no clear difference, either for extreme values or for the most probable value.

A scatter plot has been built from the maximum pressure obtained on both Concrete block and NO96 box on the 10 analogous sensors and for all tests (110 points). From the spread of the points about a diagonal, a possible trend may be detected. Such a scatter plot has been built again for total forces. Results are summarized in Figure 20. The different types of impacts are represented by different symbols of different
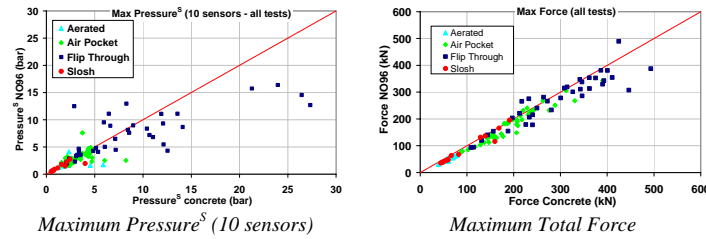
colours.

Maximum Pressure^S (10 sensors)   *Maximum Total Force*

Fig. 20 - Scatter plots Concrete block / NO96 box, for all tests

The spreading of the results for the local pressures does not allow a reliable conclusion. For the global force, even with the Flip-Through type of impact, the spreading around the diagonal is significantly reduced and most forces are larger on the Concrete block than on the NO96 box. A more refined study is nevertheless needed to explain the exceptions and confirm a possible difference in the overall behaviour of the concrete block and the NO96 box.

NUMERICAL WORK

Numerical developments

This sub-section describes the Sloshel numerical developments being carried out by BV. Malenica, Korobkin, Ten, Gazzola, Mravak, de Lauzon and Scolan, (2009) give more details.

The correct numerical modeling of the fluid-structure interactions during sloshing impacts is extremely complex, and it is fair to say that, up to now, there is no satisfactory numerical model able to treat these situations in a fully consistent manner.

The proposed general methodology is based on the composite approach "mixing" general CFD calculations, small-scale model tests, general FEM structural calculations and asymptotic theories of liquid impact. Dedicated hydro-elastic models for different impact types have been developed.

Once the impact conditions are properly identified, local hydro-elastic analysis by asymptotic fluid flow models combined with commercial FEM tools is used. The local hydro-elastic analysis is applicable only during the short duration impact stages, when the hydrodynamic loads are high and the elastic response of the insulation system is maximal. So many effects, which are of main concern in the CFD analysis, can be disregarded such as large dimensions of the tank and its real shape, real profile of the free surface at a distance from the impact region, viscosity of the fluid, its surface tension and gravity effects.

However, some effects of minor importance in the CFD analysis should be kept in the local analysis. These effects are the compressibility of the fluids, the presence of the gas above the fluid surface and in the impact region, the aeration of the fluid in the impact region, the jetting and fine details of the flow in the jet root region, the rapid increase of the wetted surface of the tank wall and the flexibility of the wall.

Short duration of the impact stage permits to simplify the local analysis and to use a combination of analytical and numerical methods instead of direct numerical calculations. Analytical part of the local analysis allows us to:

- Obtain useful formulae suitable for design needs,
- Control numerical results,
- Treat properly the coupled problem of fluid-structure interaction during the impact,
- Determine the wetted part of the wall at the same time with the fluid flow and the pressure distribution.

It is suggested to use simplified hydrodynamic models in combination with complex structural models during the impact stage because semi-analytical models of violent flows during the impact stage proved to be comparable with fully nonlinear calculations performed with high resolution in space and in time. In many cases the impact conditions and aeration of the fluid in the impact region are not well defined and small change of global conditions may lead to significant changes of the local impact conditions. Thus, attempts to reproduce all details of the flow, shape of the flow region and the fluid characteristics, have no meaning in practice.

Three main types of impacts are distinguished (Korobkin and Malenica, 2006):

(a) Slosh impact (also called Steep wave impact, Peregrine, 2003)
(b) Air Pocket impact (also called Breaking wave impact, Bagnold, 1939)
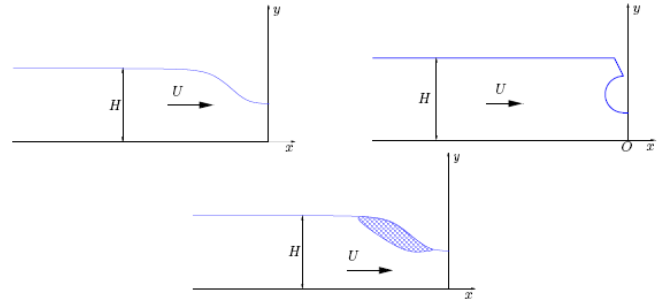(c) Aerated impact (also called Aerated fluid impact, Korobkin, 2006)

Fig. 21 - Different impact types (a - Slosh impact, b – Air-Pocket impact, c - Aerated impact)

Only the Slosh impact (Steep wave impact) and the case of acoustic approximation are briefly described. More detailed description of each particular numerical model is provided in Malenica, Korobkin, Ten, Gazzola, Mravak, de Lauzon and Scolan (2009).

Slosh Impact (Steep wave impact) occurs when the wetted area of the structure increases at a high rate and presence of the gas outside the fluid can be safely neglected (Peregrine, 2003). Close to the impact region the fluid can be in partial contact already with the structure, as in the case of steep wave impact in low filling situations, or not, as in the case of liquid impact on the ceiling.

Depending on the flow region shape and the flow field before the impact, the fluid is treated as incompressible or compressible. The fluid should be considered as compressible if the wetted area increases at very high rate, which is comparable with the sound speed in the fluid. If the rate of the impact region expansion is high but much less than the sound speed, the incompressible fluid model should be used. In this case the corresponding impact type is referred to sometimes as the Wagner type.

Acoustic approximation: in case of an almost flat impact on the wall, the situation is simplified as shown in Figure 22 where the corresponding boundary value problem for the unknown potential is also described. The fluid is assumed to be compressible.

Hydroelasticity: In case of an impact onto an elastic structure, the boundary condition at the interface changes, in order to take into account the structural deformations and their influence on fluid flow.

For the acoustic approximation, it becomes:

$$\varphi_x = w_t(y,t) \qquad (x = 0, \; 0 < y < H_w),$$
$$\varphi_x = -U + w_t(y,t) \qquad (x = 0, \; H_w < y < H),$$

where $w_t(y, t)$ is the velocity of deformation of the wall.

The additional potential related to the velocity of the structural deformations is to be introduced. The solution proposed consists in using the general FEM software for calculation of the structural natural modes while the hydrodynamic and hydro-elastic coupling parts are

processed by the normal mode decomposition method. The following types of coupled hydro-elastic equations are obtained:
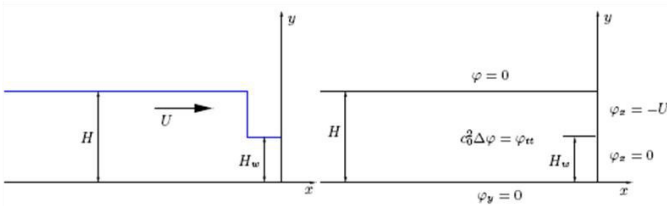

Fig. 22 - Hydraulic jump and corresponding boundary value problem

Acoustic model

$$\frac{\partial^2}{\partial t^2}\left\{MW + \int_0^t S(t-\tau)W(\tau)d\tau\right\} + KW = Q_r(t)$$

where W denotes the unknown structural response, M and K are respectively the structural mass and stiffness matrices representing the "dry" characteristics, Qr and S are the hydrodynamic actions respectively independent or dependant of the structural deformations.

Coupling with global sloshing motion: Rather simplified impact situations where the geometry and velocities are constant and simply prescribed in advance have been presented. However, impact conditions should be modified in order to reflect the overall complex fluid flow. This results in just changing the boundary conditions at the wall under the assumption of asymptotic local analysis.

These conditions become dependent on the spatial distribution of the velocity and on the different relative geometry between the structure and the liquid. From all details of the wave front approaching the vertical wall, only the shape of the wave front and its velocity before the impact stage are needed.

3D effects: The fully consistent account for 3D effects represents a major difficulty and seems to be beyond the present state of the art.
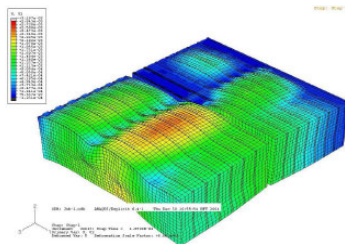

Fig. 23 - NO96 response to sloshing impact using 3D strip approach

However, good approximations considered as conservative can be adopted, using the 3D strip approach (Figure 23) based on the coupling of the 2D strip-wise hydrodynamic solutions with the full 3D structural models.

Validation of numerical tools

A large and valuable database has been built during the Sloshel project that is being used as a reference for numerical validations. Comparisons of measurements and calculations can be made at each stage of the Sloshel measurement chain from the wave paddle excitation to the structural response of the NO96 boxes and the wall. The following subsections describe first typical attempts carried out by one or other partner to simulate some links of the chain. For the time being no attempt has been made to simulate the complete chain.

Flow simulations have been simulated in two different ways: (1) Maguire, Whitworth, Oguibe, Radosavljevic and Carden (2009) describe their 2D simulation of the wave generation from the paddle to the wall, including the breaking phase and the impact on the rigid wall, with STAR-CCM+ v3.02. This is a finite volume CFD code tracking

the free surface with the HRIC (High Resolution Interface Capturing) scheme of the VOF (Volume of Fluid) technique, which allows a second-order time differencing for the free surface analyses. (2) Oger, Brosset, Guilcher, Jacquin, Deuff and Le Touzé (2009) describe their 2D impact simulation on the rigid wall with the SPH-flow software, a SPH fluid/structure solver with a fully coupled solution of the fluid-structure interaction. The simulation is carried out in a small rectangle close to the wall. The initial flow condition in this small domain and the boundary condition on the upstream boundary is obtained by an interface with FSID (Scolan, Kimmoun, Branger and Remy, 2007), a potential code developed by ECM during Sloshel project in order to mimic the shape of the breaking wave in front of the wall.

Figure 24 shows the last stage of the breaking wave for the test 74, a challenging Flip-Through impact, as obtained by STAR CCM+ and as measured by the iCAM sensors during test 74.
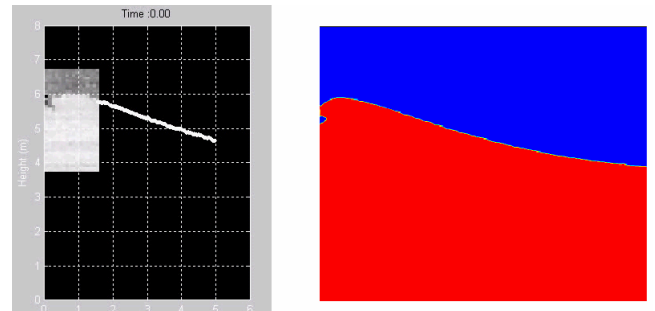

Fig. 24 – (Left) iCam data, (Right) STAR CCM+ calculation for test 74

The total impact load on the NO96 box and on the complete wall has then been calculated and compared to experimental results, as shown in Figure 25.
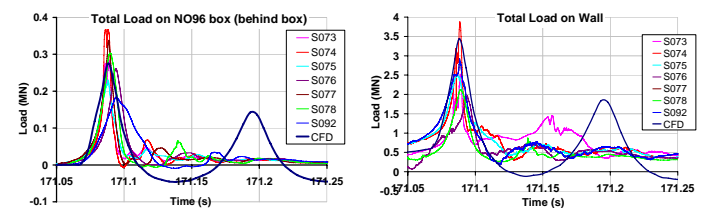

Fig. 25 - Comparison of total predicted and experimental load on the NO96 box (Left) and on the wall (Right)

The load on the NO96 box and on the wall is reasonably well predicted although oscillating forces after the impact are significantly over predicted due to the capture of a 2D air bubble as explained in Maguire, Whitworth, Oguibe, Radosavljevic and Carden (2009).

Figure 26 shows the last stage of a breaking wave as simulated by SPH-Flow, for a gas pocket impact. Pressure histories are given at four different locations facing the wave crest on the rigid wall.
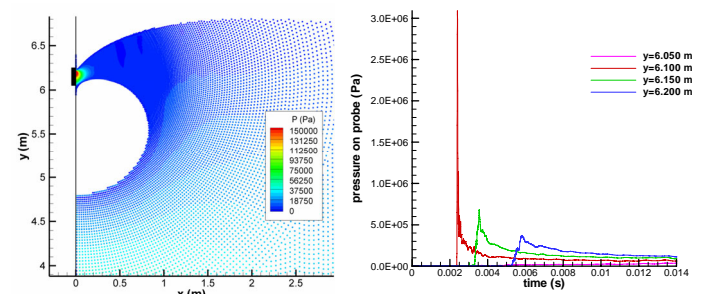

Fig. 26 - SPH-Flow simulations of an air-pocket impact by coupling with FSID. (Left) shape of the wave at wall. Colors vary with pressure (Right) pressure pulses at four heights (every 5 cm) facing the wave crest

The results shown here are to be considered as a validation of the interface with FSID potential code. It turns out to be very promising as it allows simulating very accurately any kind of breaking waves within a few hours. For more details see Oger, Brosset, Guilcher, Jacquin, Deuff and Le Touzé (2009).

Simulations of Structural responses under measured loads have been performed with different Finite Elements Software by almost all partners for the NO96 boxes by use of the material properties provided by GTT. Pillon, Marhem, Leclère and Canler (2009) present the details of their calculations with ABAQUS Software. The first validation of the model was obtained by a modal analysis. Calculated first modes are in good accordance with the experimental ones. The discrepancies on the frequencies are around 10%.

The calculated strains under the cover plates were compared with the measured ones at the locations given on Figure 6 for the test 73 (Flip Through). Moreover the force measured by the loads cells behind the NO96 box were compared to (1) the force calculated by pressure integration over the cover plate and (2) the calculated reaction. The results are shown in Figure 27.
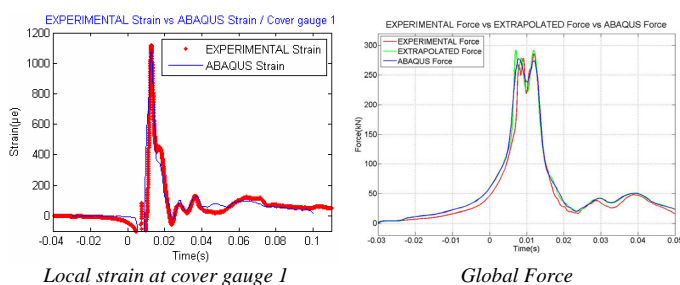

| Local strain at cover gauge 1 | Global Force |

Fig. 27 – Comparison ABAQUS calculation/Measurements – Test 73

Even the local results are in good accordance at least for the primary box. For the secondary box a conservative overestimation of the strain was noted that is probably due to the lack of coupler modeling.

Maguire, Whitworth, Oguibe, Radosavljevic and Carden (2009) have also performed successfully the Dynamic Tansient Analysis of the wall, including the propped support beams, with MSC-NASTRAN.

Fully coupled Fluid-structure interaction has been performed using the simplified semi analytical models developed by BV (see Malenica, Korobkin, Ten, Gazzola, Mravak, de Lauzon and Scolan, 2009). More sophisticated modelling using CFD has not been tried by any partner yet. Nevertheless, the SPH fluid-structure module presented above, fully integrated in the SPH-Flow platform, has been developed especially for such a purpose. Comparisons of pressures on NO96 and rigid wall for different types of impacts are intended to start soon.

CONCLUSIONS

Sloshel project can be considered as the first Full Scale Impact Tests of the NO96 containment system with wave impact conditions close to real sloshing impacts.

An extensive and sound database from 110 full-scale tests has been compiled. Each test represents an impact of a breaking wave onto a wall equipped with a fully instrumented NO96 containment system and a rigid concrete block.

Each impact has been recorded from the wave generation to the vibration of the supporting wall via the video recording of the wave, the pressure measurements, the strains and accelerations in the structure. The database gathered 185 Gigabytes of raw data. In the tests, a maximum local pressure of 26 bar and a maximum force of 5.4 tons was measured on the NO96 boxes without any structural damage.

Different kinds of wave impacts have been generated including the Flip-Through and the Air-Pocket impacts. Flip-Through induces the highest pressures over the shortest duration, showing high pressure gradients of about 10 bar over a 10 cm distance. It is very difficult to capture locally and it presents a strong sensitivity to the input conditions. The gas pocket impact presents a dual aspect: the crest of the wave induces locally high peak pressures of short duration where it hits the wall. The gas pocket itself induces a smaller and longer pressure pulse on its entire surface in contact with the wall.

The first use of this database has been for the validation of the numerical tools of the different partners. This work is just starting but has already allowed some achievements. Different approaches have been proposed within the consortium for the simulation of the wave propagation. The full CFD calculation and the coupling between a potential code and SPH Software have been tested with encouraging results. Moreover, most partners have started to tune their Finite Element models (geometrical model, material properties, boundary and bonding conditions, etc.) of the NO96 boxes in order to match their strain evaluations with the measurements for different measured impact loads. Some complete simulations including the fluid-structure coupling are now possible.

The results are still being analysed and important results are within reach concerning scaling laws, dynamic structural effects and hydro elasticity. These results will have direct consequences on the methodologies for sloshing assessment from model tests.

Numerical developments have been carried out within Sloshel project by Bureau Veritas in order to propose different models of fluid-structure interaction in typical idealized impact conditions. A strategy has to be proposed to incorporate these developments into BV's overall methodology for the assessment of sloshing within partially filled tanks of LNG carriers.

Sloshel project has also opened the way generally for the use of flume tanks or smaller wave canals for experimental research into sloshing within tanks, being particularly suited to generating repetitive wave impacts. Complementary tests at scale 1:6 have been performed within Sloshel in a smaller flume tank owned by Deltares (NL). The results, although too recent to be reported in this paper, have indicated promising insights into the impact physics.

The different systems and techniques that have been developed during Sloshel project, such as the rigid wall, the Data Acquisition and evaluation systems and the iCAM sensors, are now available to the consortium for further tests. Another programme of Full Scale Impact Tests is scheduled for beginning of 2010 with the Mark III Containment System.

ACKNOWLEDGEMENTS

REFERENCES

Bagnold, R.A., (1939). "*Interim report on wave pressure research*", Proc. Inst. Civ. Eng. Vol. 12. pp. 201-226.

Braeunig, J.-P., Brosset, L., Dias, F., Ghidaglia, J.-M. (2009). *"Phenomenological study of liquid impacts through 2D compressible two-fluid numerical simulations"*, 19th (2009) Int. Offshore and Polar Eng. Conf., Osaka, Japan, ISOPE.

Kaminski, M.L., Bogaert, H.(2009). *"Full Scale Sloshing Impact Tests"*, 19th (2009) Int. Offshore and Polar Eng. Conf., Osaka, Japan, ISOPE.

Korobkin, A.A., (2006). "*Two-dimensional problem of vertical wall impact onto partly aerated fluid*", J. Prikl. Mekh. Tekh. Phys., Vol. 47 No. 5

Korobkin, A.A. & Malenica, S., (2006). "*Local hydroelastic models for sloshing impacts*", BV Technical note, NT2912.

Maguire, J.R., Whitworth, S., Oguibe, C.N., Radosavljevic, D., Carden, E.P.(2009) *"Sloshing dynamics – numerical simulations in support of the Sloshel project"*, 19th (2009) Int. Offshore and Polar Eng. Conf., Osaka, Japan, ISOPE.

Malenica Š., Korobkin A.A., Ten I., Gazzola T., Mravak Z., De-Lauzon J. & Scolan Y.M., (2009) *"Combined semi-analytical and finite element approach for hydro structure interactions during sloshing impacts - SlosHel Project"*, 19th (2009) Int. Offshore and Polar Eng. Conf., Osaka, Japan, ISOPE.

Oger, G., Deuff, J.-B., Brosset, L., (2009). *"Simulations of hydro-elastic impacts using a parallel SPH model"*, 19th (2009) Int. Offshore and Polar Eng. Conf., Osaka, Japan, ISOPE.

Peregrine, D.H., 2003. "Water wave impact on walls.", Annual Review of Fluid Mechanics. Vol. 35. pp. 23-43

Pillon, B., Marhem , M., Leclère, G., Canler, G., (2009) *"Numerical approach for structural assessment of LNG containment systems"*, 19th (2009) Int. Offshore and Polar Eng. Conf., Osaka, Japan, ISOPE.

Scolan, Y.-M., Kimmoun, O., Branger, H., Remy, F., (2007). *"Nonlinear free surface motions close to a vertical wall. Influence of a local varying bathymetry"*, 22nd (2007) Int. Workshop on Water Waves and Floating Bodies, Plitvice, Croatia, IWWWFB.

Wang, B., Shin, Y.S., (2009) *"Full Scale Sloshing Impact Test and Coupled Fluid-Structure FE Modeling of LNG Containment System"*, 19th (2009) Int. Offshore and Polar Eng. Conf., Osaka, Japan, ISOPE.

Yataghene, M., Gavory, T., (2008) *"Catalunya Spirit Incident – Enhancement in the knowledge of Liquid Motions in membrane LNGC tanks"* SIGTTO panel meeting (restricted to SIGTTO members only), Bruneï, Oct. 2008.